131.43, 131.40, 131.2, 131.0, 130.6, 129.9, 129.6, 129.55, 129.53, 129.4, 129.3, 129.2, 129.1, 129.02, 128.98, 128.7, 128.4, 128.32, 128.27, 128.21, 128.15, 127.8, 127.7, 127.5, 127.4, 126.9, 126.4, 126.1, 125.5, 125.3, 125.2, 125.1, 125.0, 124.7, 124.6, 124.4, 124.3, 124.24, 124.20, 124.04, 123.95, 123.9, 123.8, 123.6, 122.4, 121.1, 46.6, 37.1, 36.6, 36.5, 35.9, 34.9, 34.3, 34.2, 34.13, 34.11, 34.06, 34.0, 33.9, 33.8, 33.6, 32.3, 31.7, 31.67, 31.64, 31.59, 31.58, 31.5, 31.3, 31.2, 31.1, 30.6, 15.4 (minor), 15.3; MS (+FAB)1598 (M + H, 24), 1408 (100).

Acknowledgment. S.F.P. is grateful to the National Science Foundation for a Presidential Young Investigator Award (Grant No. CHE-8552735) and to Eli Lilly and Co. and Rohm and Haas Co. for financial support of this work.

Supplementary Material Available: Full characterization of compounds **2a**, **3a**,**c**-**e**, **4b**, **5**, **7**, **8**, **10**, **11**, **13**, **14**, **16** and **18**, experimental details of the mass spectrometry and two-dimensional NMR spectroscopy experiments, one-dimensional ^{1}H NMR spectrum of **3b** at -43 °C with all resonances labeled according to Figure 5, COSY spectrum of **3b** at -45 °C, ROESY spectrum of **3b** at -43 °C, and difference NOE spectrum of **3b** at -40 °C (35 pages). Ordering information is given on any current masthead page.

Nonplanar Porphyrins. X-ray Structures of (2,3,7,8,12,13,17,18-Octaethyl- and -Octamethyl-5,10,15,20-tetraphenylporphinato)zinc(II)

Kathleen M. Barkigia,[1a] M. Dolores Berber,[1b] Jack Fajer,*[,1a] Craig J. Medforth,[1b] Mark W. Renner,[1a] and Kevin M. Smith*[,1b]

Contribution from the Department of Applied Science, Brookhaven National Laboratory, Upton, New York 11973, and Department of Chemistry, University of California, Davis, California 95616. *Received May 7, 1990*

Abstract: X-ray structures of the peripherally crowded porphyrins, (2,3,7,8,12,13,17,18-octaethyl-5,10,15,20-tetraphenylporphinato)Zn(II)-3MeOH solvate (ZnOETPP·3MeOH) and (2,3,7,8,12,13,17,18-octamethyl-5,10,15,20-tetraphenylporphinato)Zn(II)-pyridine-2HCCl$_3$ (ZnOMTPP·py·2HCCl$_3$) are reported. Both molecules are severely nonplanar and assume saddle shapes. ^{1}H NMR data confirm that the conformational distortions are maintained in solution. The consequences of distorting the macrocycles are significant: optical, redox, basicity, and excited-state properties are altered in agreement with previous theoretical calculations. These results form part of an expanding body of structural information that clearly demonstrates that porphinoid skeletons are flexible and that distortions of the macrocycles can be imposed by steric interactions in vitro and in vivo. Conformational variations thus provide an attractively simple mechanism for modulating a wide range of physical and chemical properties of porphyrinic chromophores and prosthetic groups in vitro and in vivo. Crystallographic data. $ZnN_4C_{60}H_{60}\cdot 3CH_3OH$: triclinic space group $P\bar{1}$, a = 14.017 (10) Å, b = 16.494 (7) Å, c = 13.073 (9) Å, α = 96.12 (5)°, β = 107.48 (6)°, γ = 105.23 (6)°, V = 2724.5 Å^3, Z = 2; R_F and R_{wF} = 0.062, based on 4281 reflections with $F_o > 2\sigma F_o$; T = 200 K. $ZnN_4C_{52}H_{44}\cdot C_5D_5N\cdot 2HCCl_3$: monoclinic space group $C2/c$, a = 22.411 (23) Å, b = 12.552 (10) Å, c = 19.287 (12) Å, β = 98.66 (10)°, V = 5363.6 Å^3, Z = 4; R_F = 0.060 and R_{wF} = 0.061, based on 1722 reflections with $F_o > 2\sigma F_o$; T = 298 K.

Introduction

Recent structural data for porphyrins, chlorins, bacteriochlorins, and isobacteriochlorins as isolated molecules and in proteins illustrate the considerable flexibility of the chromophores and the significant distortions that can be imposed upon porphinoid macrocycles by crystal packing, steric effects, or protein constraints.[2-8] Particularly intriguing are the multiple conformations reported for the bacteriochlorophylls *b* that comprise the primary donor or special pair of the reaction center of *Rhodopseudomonas viridis*,[7] and for the bacteriochlorophylls *a* that constitute a light-harvesting antenna complex of *Prosthecochloris aestuarii*.[8] Theoretical calculations[6,9] indicate that conformational variations would shift the highest occupied (HOMO) and lowest unoccupied

(1) (a) Brookhaven National Laboratory. (b) University of California.
(2) For a review, see: Scheidt, W. R.; Lee, Y. J. *Struct. Bonding (Berlin)* **1987**, *64*, 1.
(3) Chow, H. C.; Serlin, R.; Strouse, C. E. *J. Am. Chem. Soc.* **1975**, *97*, 7230. Serlin, R.; Chow, H. C.; Strouse, C. E. *Ibid.* **1975**, *97*, 7237. Kratky, C.; Dunitz, J. D. *Acta Crystallogr., Sect. B* **1975**, *B32*, 1586; **1977**, *B33*, 545. Kratky, C.; Dunitz, J. D. *J. Mol. Biol.* **1977**, *113*, 431. Kratky, C.; Isenring, H. P.; Dunitz, J. D. *Acta Crystallogr., Sect. B* **1977**, *B33*, 547. Smith, K. M.; Goff, D. A.; Fajer, J.; Barkigia, K. M. *J. Am. Chem. Soc.* **1982**, *104*, 3747; **1983**, *105*, 1674. Fajer, J.; Barkigia, K. M.; Fujita, E.; Goff, D. A.; Hanson, L. K.; Head, J. D.; Horning, T.; Smith, K. M.; Zerner, M. C. In *Antennas and Reaction Centers of Photosynthetic Bacteria*; Michel-Beyerle, M. E., Ed.; Springer-Verlag: Berlin, 1985; p 324.
(4) Barkigia, K. M.; Fajer, J.; Chang, C. K.; Young, R. *J. Am. Chem. Soc.* **1984**, *106*, 6457. Wadtschatka, R.; Kratky, C.; Juan, B.; Heinzer, J.; Eschenmoser, A. *J. Chem. Soc., Chem. Commun.* **1985**, 1604. Barkigia, K. M.; Gottfried, D. S.; Boxer, S. G.; Fajer, J. *J. Am. Chem. Soc.* **1989**, *111*, 6444.
(5) Barkigia, K. M.; Fajer, J.; Chang, C. K.; Williams, G. J. B. *J. Am. Chem. Soc.* **1982**, *104*, 315. Suh, M. P.; Swepston, P. N.; Ibers, J. A. *J. Am. Chem. Soc.* **1984**, *106*, 5164. Kratky, C.; Waditschatka, R.; Angst, C.; Johansen, J. E.; Plaquerent, J. C.; Schreiber, J.; Eschenmoser, A. *Helv. Chim. Acta* **1985**, *68*, 1312. Strauss, S. H.; Silver, M. E.; Long, K. M.; Thompson, R. G.; Hudgens, R. A.; Spartalian, K.; Ibers, J. A. *J. Am. Chem. Soc.* **1985**, *107*, 4207. Stolzenberg, A. M.; Glazer, P. A.; Foxmann, B. M. *Inorg. Chem.* **1986**, *25*, 983. Brennan, T. D.; Scheidt, W. R.; Shelnutt, J. A. *J. Am. Chem. Soc.* **1988**, *110*, 3919.
(6) Barkigia, K. M.; Chantranupong, L.; Smith, K. M.; Fajer, J. *J. Am. Chem. Soc.* **1988**, *110*, 7566.
(7) Deisenhofer, J.; Michel, H. *Science* **1989**, *245*, 1463, and references therein.
(8) Tronrud, D. E.; Schmid, M. F.; Matthews, B. W. *J. Mol. Biol.* **1986**, *188*, 443.
(9) Gudowska-Nowak, E.; Newton, M. D.; Fajer, J. *J. Phys. Chem.* **1990**, *94*, 5795.

0002-7863/90/1512-8851$02.50/0

(LUMO) molecular orbitals of the chromophores and thereby modulate their redox and light-absorption properties. Such effects, in conjunction with additional interactions with nearby proteins residues,[6,10] would thus offer attractively simple rationales for the multiple absorption maxima observed in the low-temperature optical spectra of the *P. aestuarii* antenna,[9] and for the asymmetry in the oxidized special pair,[11] its triplet state,[12] and the vectorial electron flow in the *R. viridis* reaction center.[6,10]

We have recently tested the above concept by demonstrating that a sterically distorted porphyrin, (2,3,7,8,12,13,17,18-octaethyl-5,10,15,20-tetraphenylporphinato)Zn(II) (ZnOETPP), exhibits optical and redox properties in solution consonant with theory.[6] The compound is easier to oxidize and absorbs light at lower energies than more planar Zn porphyrins, in agreement with the calculated destabilization of the HOMO and the resulting smaller gap between the HOMO and LUMO.[6] We present here X-ray diffraction results for ZnOETPP and for the corresponding octamethyl derivative, ZnOMTPP, that illustrate the severe saddle distortions caused by crowding of the peripheral substituents. We also provide NMR data that establish that the distortions are maintained in solution and discuss possible consequences and implications of conformational variations on the properties of porphyrin derivatives in vitro and in vivo.

Methods

ZnOETPP[13] and ZnOMTPP[14] were synthesized by preparing the corresponding porphyrinogens, oxidizing the latter with quinone, and inserting Zn by using $Zn(OAc)_2$.

A 2-L three-necked round-bottom flask fitted with a reflux condenser and nitrogen inlet port was filled with 1 L of freshly distilled dichloromethane. Benzaldehyde (1 mL, 0.01 mol) and 3,4-diethylpyrrole (1.23 g, 0.01 mol) were added, and the solution was stirred at room temperature under a slow steady stream of nitrogen gas. After 15 min, $BF_3{\cdot}OEt_2$ (0.14 g, 0.001 mol) was added, the reaction vessel was shielded from ambient light, and the mixture was stirred for 1 h at room temperature. The solvent was evaporated under reduced pressure, and the oily residue was taken up in methanol and kept in the freezer overnight. The solution was transferred to centrifuge tubes with more methanol. A white solid separated from the dark pink solution and was recrystallized with a dichloromethane–methanol mixture to yield 1.41 g (67%) of 2,3,7,8,12,13,17,18-octaethyl-5,10,15,20-tetraphenylporphyrinogen.

2,3-Dichloro-5,6-dicyano-1,4-benzoquinone (108 mg, 0.48 mmol, 4 equiv) was added all at once to a stirred solution of the porphyrinogen (100 mg, 0.12 mmol) in 25 mL of dry toluene or dichloromethane. The solution turned dark pink instantly and was refluxed under nitrogen for 30 min to give a green solution. The solvent was evaporated to dryness and the residue was taken up in dichloromethane. An alumina column (Brockman grade III, 3 × 10 cm) eluting with 2% methanol in dichloromethane was used to separate the porphyrin as a major green fraction. The solvent was removed to afford a green solid, which was crystallized from CH_2Cl_2–MeOH as green crystals of the diprotonated porphyrin. Some of the porphyrin became insoluble even in methanol and was left at the top of the column. This porphyrin was dissolved in a KOH–ethanol (0.5%) solution and then filtered. The filtrate and the product collected by column chromatography were mixed and evaporated under vacuum. The residue was taken up in dichloromethane, and the porphyrin was crystallized as the free base by using a 0.2% ethanolic solution of KOH. The product was dried in a vacuum oven to afford 82 mg (82% yield, based on porphyrinogen) of blue needles. mp > 300 °C. λ_{max} (CH_2Cl_2): nm ($\epsilon \times 10^{-3}$), 446 (159.7), 548 (19.1, br), 588 (16.8, br), 634 (sh), 686 (16.1, br). ^{1}H NMR ($CDCl_3$, 300 MHz): δ 8.32 (m, 8 H, *o*-Ar-H), 7.72 (m, 4 H, *p*-Ar-H), 7.66 (m, 8 H, *m*-Ar-H), 2.61 and 1.90 (m br, 16 H, CH_2), 0.43 (t br, 24 H, CH_3), −2.0 (s br, 2 H, NH).

The free base porphyrin (82 mg, 0.10 mmol) was dissolved in a saturated solution of $Zn(OAc)_2$ in 20 mL of DMF containing some NaOAc (4:1). The mixture was refluxed under nitrogen and monitored spectrophotometrically until there was no residual Soret band from the starting compound. Dichloromethane (20 mL) was added when the reaction vessel reached room temperature. The mixture was then washed with brine (3 × 50 mL) and the metalated porphyrin was extracted into dichloromethane. The organic solution was then dried over Na_2SO_4 and the solvent evaporated under reduced pressure. Crystallization with dichloromethane and methanol afforded the zinc porphyrin as green metallic plates in almost quantitative yield. The crystals contained three molecules of methanol per porphyrin. λ_{max} (CH_2Cl_2): nm ($\epsilon \times 10^{-3}$), 454 (202.0), 586 (13.1), 637 (5.5). λ_{max} (CH_2Cl_2 + pyridine, 9:1): nm ($\epsilon \times 10^{-3}$), 468 (230.3), 610 (5.9), 660 (5.7). λ_{max} (CH_2Cl_2 + CH_3OH, 9:1): nm ($\epsilon \times 10^{-3}$), 464 (170.0), 609 (15.7), 655 (15.0). ^{1}H NMR ($CDCl_3$, 300 MHz): δ 8.33 (m, 8 H, *o*-Ar-H), 7.72 (m, 4 H, *p*-Ar-H), 7.67 (m, 8 H, *m*-Ar-H), 2.53 and 2.01 (m, 16 H, CH_2), 0.43 (t, 24 H, CH_3).

The octamethyl derivative was prepared in a similar fashion starting with 3,4-dimethylpyrrole. The Zn complex was crystallized from pyridine–chloroform. The crystals contained one molecule of pyridine and two molecules of chloroform per porphyrin. λ_{max} (CH_2Cl_2): nm ($\epsilon \times 10^{-3}$), 442 (160.0), 574 (13.1), 630 (5.5). λ_{max} (CH_2Cl_2 + pyridine): nm ($\epsilon \times 10^{-3}$), 458 (83.9), 595 (9.0), 646 (7.7). ^{1}H NMR ($CDCl_3$, 300 MHz): δ 8.18 (m, 8 H, *o*-Ar-H), 7.64 (m, 4 H, *p*-Ar-H), 7.67 (m, 8 H, *m*-Ar-H), 1.86 (s, 24 H, CH_3).

Proton NMR spectra were recorded at 300 MHz on a General Electric QE 300 spectrometer at UCD. Temperature-dependent studies were confirmed at BNL using a Bruker AM 300 MHz spectrometer. (The data reported are those obtained on the GE spectrometer.) ZnOETPP undergoes some demetalation in benzene or 1,1,2,2-tetrachloroethane. Neat pyridine yielded stable solutions and provided a suitable temperature range. Spectra were recorded in 5 mM solutions of the porphyrin in pyridine-d_5 (>99.96 atom % D, Aldrich) containing TMS as internal standard. Typical experimental conditions included a spectral window of 4000 Hz, 16K data points, and a 90° pulse. The variable-temperature unit of the QE300 spectrometer was calibrated with ethylene glycol and methanol standard samples[15] and was found to be accurate to ±2 °C over the range −85 to +110 °C.

Crystallography. ZnOETPP crystallized from CH_2Cl_2–CH_3OH with three methanols of solvation ($ZnN_4C_{60}H_{60}{\cdot}3CH_3OH$) in the triclinic space group $P\bar{1}$, with a = 14.017 (10) Å,[16] b = 16.494 (7) Å, c = 13.073 (9) Å, α = 96.12 (5)°, β = 107.48 (6)°, γ = 105.23 (6)°, V = 2724.5 Å^3, and Z = 2. Data were collected at 200 K on an Enraf-Nonius CAD4 diffractometer with graphite-monochromated Mo Kα radiation in the scan range $2 \le \theta \le 22.5°$. Of the 8029 reflections ($h \pm k \pm l$) measured, 6924 were unique and 4281 had $F_o > 2\sigma F_o$. (Data were corrected for Lorentz and polarization effects but not for absorption due to a malfunction of the temperature controller.) The positions of 52 of the 65 atoms of the macrocycle were determined from MULTAN 78.[17] The other atoms and the three methanol molecules were determined from successive difference maps. Hydrogens were included in the model in calculated positions, except for those in the methanols. Anisotropic refinement of all non-hydrogen atoms using full-matrix least-squares routines with anomalous terms[18] for Zn yielded R_F = 0.062 and R_{wF} = 0.062.

ZnOMTPP crystallized from pyridine-d_5–chloroform with one py ligand and two molecules of $HCCl_3$ of solvation ($ZnN_4C_{52}H_{44}{\cdot}C_5D_5N{\cdot}2HCCl_3$) in the monoclinic space group $C2/c$ with a = 22.411 (23) Å, b = 12.552 (10) Å, c = 19.287 (12) Å, β = 98.66 (10)°, V = 5363.6 Å^3, and Z = 4. Data were collected at 298 K with graphite-monochromated Cu Kα radiation in the scan range $2 \le \theta \le 50°$. Of the 3235 reflections measured excluding those systematically absent due to the C-centering, 2926 were unique and 1722 had $F_o > 2\sigma F_o$. Standard Lorentz and polarization corrections were applied as well as a decay correction[19] because the compound deteriorated during data collection. The decay precluded measurements of a ψ scan for absorption corrections. The positions of 25 of the 29 atoms that comprise half the macrocycle were determined by MULTAN 78. The other atoms, the axial pyridine, and the chloroform of solvation were located from difference Fourier maps. Hydrogens were included in the model in calculated positions, except for

(10) Plato, M.; Mobius, K.; Michel-Beyerle, M. E.; Bixon, M.; Jortner, J. *J. Am. Chem. Soc.* **1988**, *110*, 7279.
(11) Lendzian, F.; Lubitz, W.; Scheer, J.; Hoff, A. J.; Plato, M.; Trankle, E.; Mobius, K. *Chem. Phys. Lett.* **1988**, *148*, 377.
(12) Norris, J. R.; Budil, D. E.; Gast, P.; Chang, C.-H.; El-Kabbani, O.; Schiffer, M. *Proc. Natl. Acad. Sci. U.S.A.* **1989**, *86*, 4335.
(13) Evans, B.; Smith, K. M.; Fuhrhop, J.-H. *Tetrahedron Lett.* **1977**, 443.
(14) Dolphin, D. *J. Heterocycl. Chem.* **1970**, *7*, 275.
(15) van Geet, A. L. *Anal. Chem.* **1970**, *42*, 679.
(16) The figures in parentheses are the standard deviations of the least significant figure here and throughout the paper.
(17) Main, P.; Hill, S. E.; Lessinger, L.; Germain, G.; Declercq, J. P.; Woolfson, M. M. *Multan 78, A System of Computer Programs for the Automatic Solution of Crystal Structures from X-ray Diffraction Data*; University of York, England, and University of Louvain, Belgium, 1978.
(18) Scattering factors for non-hydrogen atoms are taken from: Cromer, D. T.; Mann, J. B. *Acta Crystallogr., Sect. A* **1968**, *A24*, 321. Scattering factors for hydrogens are from: Stewart, R. F.; Davidson, E. R.; Simpson, W. T. *J. Chem. Phys.* **1965**, *42*, 3175. The anomalous components are taken from: *International Tables for X-ray Crystallography*; Kynoch Press: Birmingham, England, 1974; Vol. IV, pp 148–151.
(19) Churchill, M. R.; Kalra, K. L. *Inorg. Chem.* **1974**, *13*, 1427 (footnote 12).

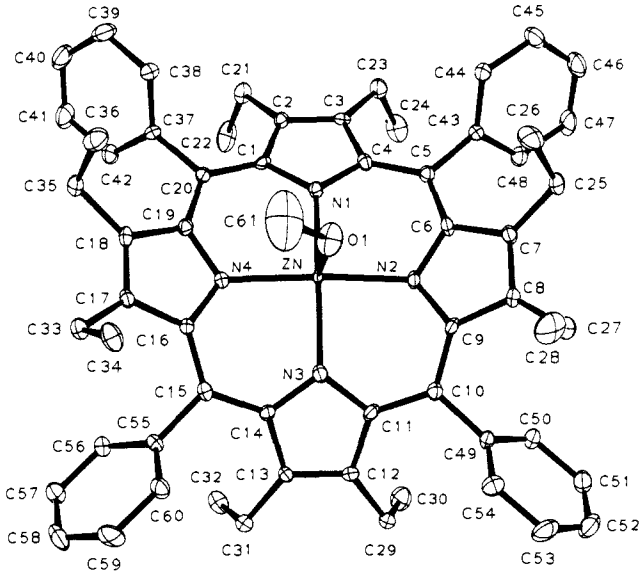

Figure 1. Molecular structure and atom names of ZnOETPP·MeOH. Hydrogens are omitted for clarity. Thermal ellipsoids are drawn to enclose 50% probability.

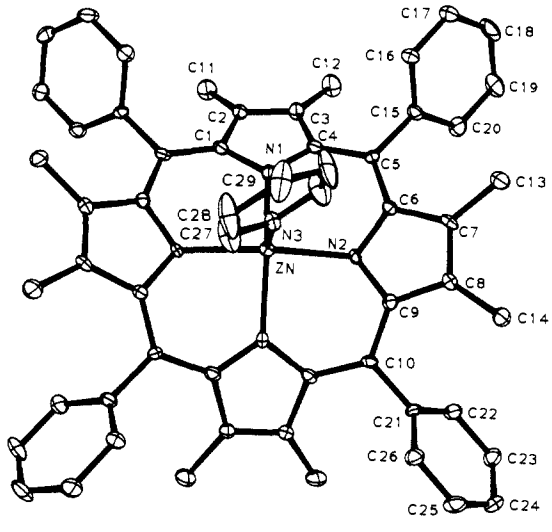

Figure 2. Molecular structure and atom names of ZnOMTPP·py. Hydrogens are omitted for clarity. Thermal ellipsoids are contoured at the 50% level.

those on the solvent molecules. Anisotropic refinement of all non-hydrogen atoms using full-matrix least-squares procedures with anomalous terms for Zn and Cl yielded $R_F = 0.060$ and $R_{wF} = 0.061$. The programs used are locally modified VAX versions of the CRYSNET package and other in-house programs.[20]

Final positional parameters for the atoms of ZnOMTPP and ZnOETPP, and final anisotropic thermal parameters and structure factor amplitudes for both compounds, are included in the supplementary material.

Crystallographic Results

ZnOETPP and ZnOMTPP crystallize with the Zn ligated by methanol (MeOH) and pyridine (py), respectively. Unlike most pentacoordinated ZnOEP's and ZnTPP's, of which the present compounds are hybrids, ZnOETPP and ZnOMTPP are strikingly nonplanar and exhibit severe S_4 saddle shapes.

The molecular structures and atom names for ZnOETPP·MeOH and ZnOMTPP·py are presented in Figures 1 and 2, respectively. Each pyrrole ring with its β-alkyl substituents is displaced alternately up and down, and the phenyl rings are rotated

(20) Berman, H. M., Bernstein, F. C., Bernstein, H. J., Koetzle, T. F., Williams, G. J. B., Eds.; Informal Report BNL 21714; Brookhaven National Laboratory, Upton, NY, 1976.

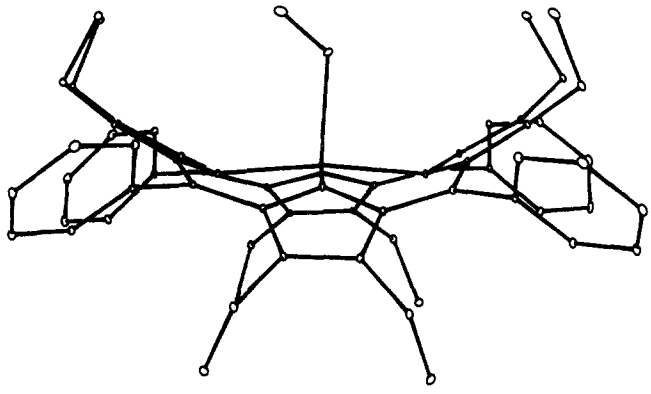

Figure 3. Edge-on view of ZnOETPP·MeOH that illustrates the deformation of the porphyrin skeleton and the orientations of substituents.

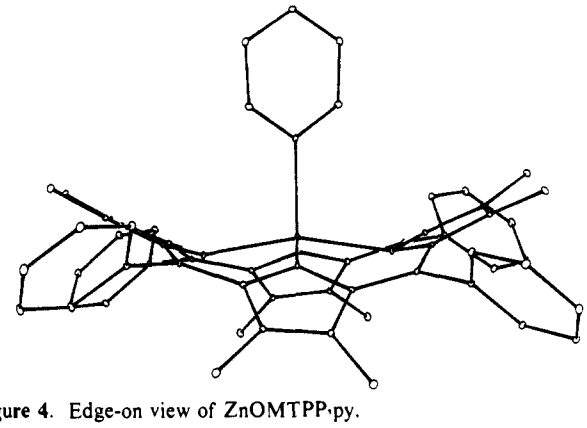

Figure 4. Edge-on view of ZnOMTPP·py.

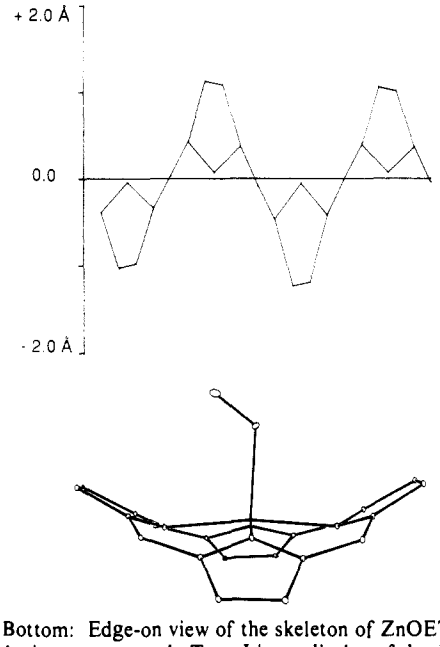

Figure 5. Bottom: Edge-on view of the skeleton of ZnOETPP·MeOH with the substituents removed. Top: Linear display of the deviations of the 24 atoms of the macrocycle from a plane defined by the four nitrogens. (The horizontal axis is not to scale.)

into the macrocycle plane to minimize contacts between the substituents. These effects are illustrated in Figures 3 and 4, which display the molecules viewed edge-on. The significant distortions of the porphyrin skeletons themselves are shown in Figures 5 and 6, which also present the deviations of the 24 atoms that comprise each porphyrin ring from a plane defined by the four nitrogens. The skeletal deformations are equally striking when viewed as the perpendicular displacements of the atoms from the mean plane of the 24-atom core (Figures 7 and 8). Note that C_β atoms of adjacent pyrrole rings are alternately displaced above and below

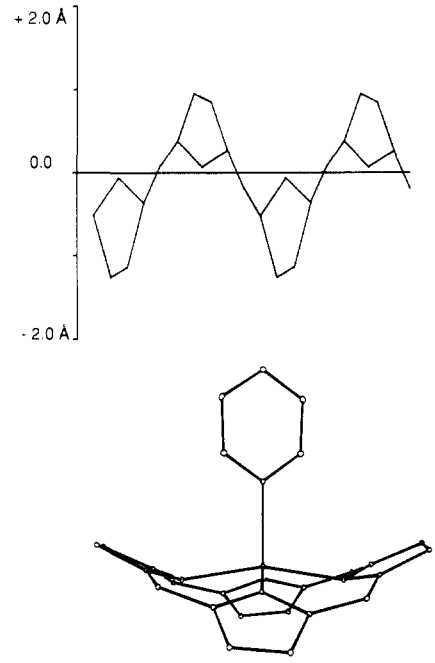

Figure 6. Bottom: Edge-on view of the skeleton of ZnOMTPP·py. Top: Deviations of the 24 atoms of the macrocycle from the plane defined by the four nitrogens. The whole molecule is shown for completeness although the halves are symmetry-related.

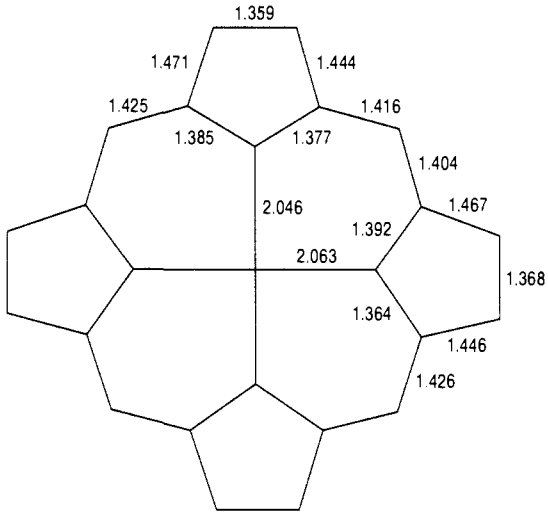

Figure 7. Displacements of the 24 atoms that comprise the ZnOETPP porphyrin core from the mean plane of the 24 atoms, in units of 0.01 Å.

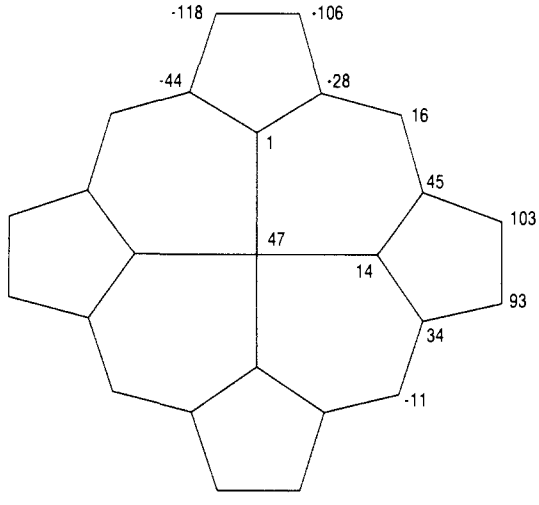

Figure 8. Displacements of the atoms of the ZnOMTPP core from the mean plane of the macrocycle, in units of 0.01 Å.

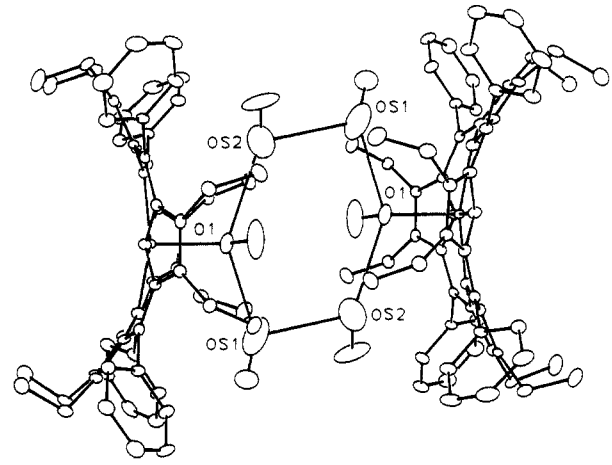

Figure 9. Bond distances in ZnOETPP, in Å. esd's are 0.008 Å for a typical C–C bond and 0.005 Å for the Zn–N distances.

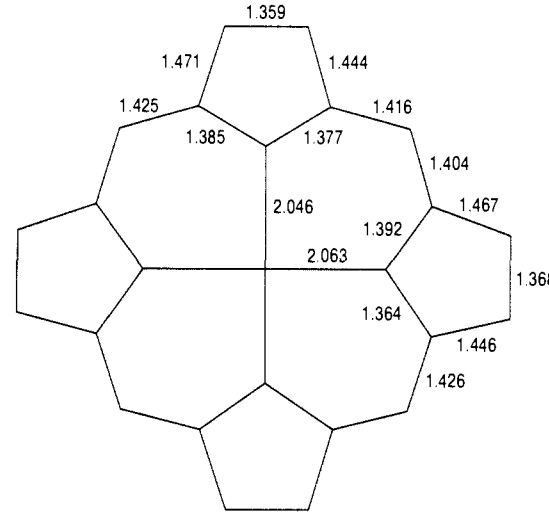

Figure 10. Bond distances in ZnOMTPP, in Å. esd's are 0.009 Å for C–C bonds and 0.006 Å for Zn–N distances.

the macrocycle planes by more than 1 Å. Adjacent pyrrole rings in ZnOMTPP are tilted 38.6° while those in ZnOETPP lie at angles of 36.5–41.3° to each other. Individually, each pyrrole ring in both structures is planar with the largest deviation of 0.043 (6) Å at N2 of ZnOMTPP and 0.039 (5) Å at N2 of ZnOETPP. The $C_\alpha C_\beta C_\beta C_\alpha$ dihedral angles are less than 2° in all the pyrrole rings.

As expected for saddle deformations,[21] the dihedral angles of the phenyl rings with the nitrogen planes are smaller than normally observed for more planar macrocycles. The angles are 43.9 and 43.6° for ZnOMTPP and 47.7, 46.9, 45.1, and 42.3° in ZnOETPP. There are no unreasonably short intramolecular contacts between the substituents, as the saddle conformations minimize these approaches. In ZnOMTPP, the shortest contact between *o*-phenyl and methyl carbons is 3.14 Å (C13–C20) while the shortest analogous distance in ZnOETPP, C33–C56, is 3.25 Å.

The nonplanarity of the macrocycles is clearly *not* due to intermolecular interactions. The shortest intermolecular contact, excluding the solvent molecules of ZnOMTPP (vide infra), is 3.67 Å between C17 and C26 of the phenyl rings. Furthermore, the phenyl rings of adjacent molecules do not overlap: their centers are over 5 Å from each other. There are also no intermolecular contacts between ring atoms less than 4 Å and thus there is no evidence of π–π interactions between adjacent molecules that might cause distortions of the macrocycle.[21] Indeed, the closest center-to-center approach of neighboring pyrrole rings is 6.99 Å.

(21) For a review, see: Scheidt, W. R.; Lee, Y. H. *Struct. Bonding (Berlin)* **1987**, *64*, 1.

Table I. Comparisons of Selected Distances and Angles in ZnOMTPP and ZnOETPP with Average Porphyrin Values[a]

	ZnOMTPP	ZnOETPP	average[b]
	Distances, Å		
C_α–N	1.380 (6)	1.371 (4)	1.379 (6)
C_α–C_β	1.457 (7)	1.461 (2)	1.443 (5)
C_β–C_β	1.364 (9)	1.370 (7)	1.354 (10)
C_α–C_m	1.418 (5)	1.416 (3)	1.390 (11)
C_m–C_ϕ	1.487 (9)	1.494 (2)	1.499 (5)
	Angles, deg		
NMN	88.0 (2)	89.4 (4)	89.7 (2)
$C_\alpha NC_\alpha$	106.3 (6)	107.7 (5)	105.5 (3)
MNC_α	124.0 (12)	122.9 (6)	127.2 (1)
$NC_\alpha C_m$	122.7 (6)	122.4 (2)	125.7 (2)
$NC_\alpha C_\beta$	109.8 (6)	109.2 (3)	110.2 (2)
$C_\beta C_\alpha C_m$	127.4 (5)	128.2 (2)	124.2 (1)
$C_\alpha C_m C_\alpha$	123.0 (6)	124.4 (4)	123.8 (3)
$C_\alpha C_\beta C_\beta$	106.9 (6)	106.8 (2)	107.0 (1)

[a] The estimated standard deviation of the mean was calculated as $[\sum m(ml_m - \bar{l})^2/m(m-1)]^{1/2}$ for more than two contributors and as the average of the esd's for two contributors. [b] See ref 23.

Similarly for ZnOETPP, there are no porphyrin contacts less than 4 Å and the closest distance between symmetry-related phenyl rings is 5.00 Å.

For both compounds, bonds distances in the macrocycles (Figures 9 and 10) and Zn–N distances are insensitive to the crowded periphery. The Zn–N bonds average 2.055 (6) Å in ZnOMTPP and 2.063 (5) Å in ZnOETPP and are consistent with literature values that vary from 2.051 (3) to 2.076 (9) Å in pentacoordinated Zn porphyrins.[22] A comparison of some average distances for these compounds in Table I further illustrates this invariance. Noteworthy are the unshortened meso carbon to phenyl carbon bonds of 1.487 (9) Å in ZnOMTPP and 1.494 (2) Å in ZnOETPP, indicating no increased conjugation of the phenyl rings with the macrocycle, in spite of the phenyl rotations into the porphyrin plane.

The effects of the adjacent alkyl and phenyl groups are mainly reflected in the bond angles, Table I. As the pyrroles tilt to prevent unfavorable contacts between substituents, the C_β–C_α–C_m angles increase with a concomitant decrease in the N–C_α–C_m and M–N–C_α angles. The angles change by 3–4° from those in "average" structures described by Hoard.[23] The remainder of the angles in both structures are essentially unperturbed.

Both molecules crystallize with well-ordered molecules of solvation. ZnOMTPP is ligated by py and lies on a 2-fold axis that passes through the Zn and C29 and N3 of the py. In addition, the lattice contains two $HCCl_3$ molecules per Zn. The asymmetric unit of ZnOETPP includes one complete porphyrin molecule and three MeOH molecules, one of which is bound to the Zn; the other two methanols are each hydrogen bonded to the ligand (vide infra).

The Zn atom is displaced 0.39 Å from the plane of the nitrogens in ZnOMTPP and 0.22 Å in ZnOETPP. Compared to other Zn porphyrins with nitrogenous ligands,[21] the Zn displacement in ZnOMTPP is quite ordinary. The metal displacement in ZnOETPP agrees with those observed in the disordered ZnTPP·H_2O[24] and the dimeric cation $(ZnOEP{\cdot}H_2O)_2{\cdot}2ClO_4$, where H_2O is the axial ligand.[22]

As noted above, the average Zn–N distances of 2.055 (6) Å in ZnOMTPP and 2.063 (5) Å in ZnOETPP are typical of five-coordinate Zn porphyrins. The Zn–ligand distances are normal as well: the Zn–O distance of 2.226 (5) Å is comparable to that of 2.20 (6) Å in ZnTPP·H_2O,[24] but shorter than the 2.380 (2) Å reported for the loosely bound tetrahydrofuran molecules in the six-coordinate $ZnTPP(THF)_2$.[25]

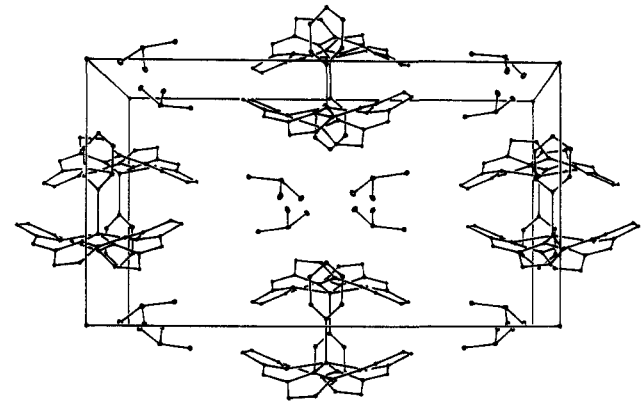

Figure 11. Illustration of the packing in ZnOMTPP·py·$2HCCl_3$. Ethyl and phenyl substituents have been removed for clarity.

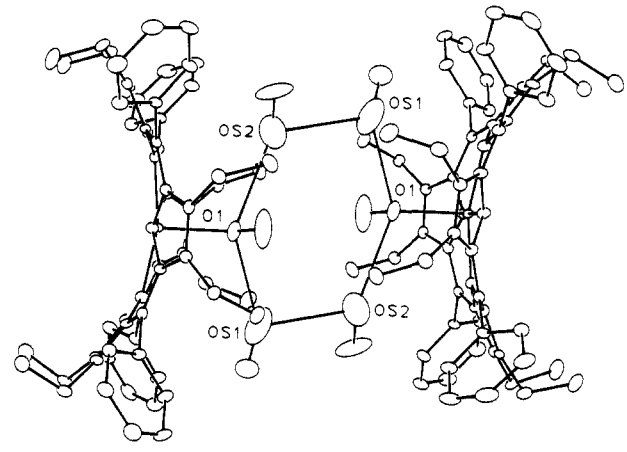

Figure 12. Illustration of the six-membered oxygen ring formed by hydrogen bonding between the methanol ligated to the ZnOETPP, the two methanols of solvation (OS1 and OS2), and the three methanols associated with an inversion-related porphyrin. Distances: O1–OS1, 3.16 Å; O1–OS2, 2.89 Å; OS1–OS2, 2.96 Å.

The Zn–Npy distance of 2.144 (9) Å in ZnOMTPP also falls within the range of 2.143 (4)–2.200 (3) Å found in other pyridine-ligated Zn porphyrins.[21]

The py ligand of ZnOMTPP is oriented 29.7° with respect to the N2–N4 direction and is constrained by symmetry to lie perpendicular to the plane of the nitrogens. Its orientation is probably governed by a combination of factors. As suggested by Hoard,[23] the interactions of the α-protons of the py (deuterons in this case) with the core are minimized when the dihedral angle between opposite nitrogens and the axial ligand approaches 45°. Secondly, with the implicit steric bulk of the macrocycle, the pyridine adjusts to prevent unfavorable contacts with the phenyl rings. Finally, the pyridine must accommodate the two $HCCl_3$ molecules, while lie 3.96 Å away from it.

Although the molecules of ZnOMTPP are well-separated, they pack in pairs that are centrosymmetrically related, with a Zn–Zn distance of 10.27 Å. The $HCCl_3$ molecules act as "spacers" between pairs and align with the chlorines directed away from the convex side of the molecule and with the hydrogens pointing into the porphyrin (Figure 11).

The coordinated MeOH in ZnOETPP is skewed. The O1–Zn–N1, O1–Zn–N2, O1–Zn–N3, and O1–Zn–N4 angles are 94.7 (2), 96.2 (2), 100.8 (2), and 97.6 (2)°, respectively, and the Zn–O1–C61 angle is 127.0 (6)°. Since the ethyl groups of adjacent pyrrole rings lie alternately down and up, the MeOH nestles in the cavity between the "up" ethyl groups on rings II and IV. Surprisingly, the oxygen of the hydroxyl group, O1, is hydrogen-bonded to the oxygens, OS1 and OS2, of the methanols of

(22) Song, H.; Reed, C. A.; Scheidt, W. R. *J. Am. Chem. Soc.* **1989**, *111*, 6867. Spaulding, L. D.; Eller, P. G.; Bertrand, J. A.; Felton, R. H. *J. Am. Chem. Soc.* **1974**, *96*, 982.

(23) Hoard, J. L. In *Porphyrins and Metalloporphyrins*; Smith, K. M., Ed.; Elsevier: Amsterdam, 1975; p 317.

(24) Glick, M. D.; Cohen, G. H.; Hoard, J. L. *J. Am. Chem. Soc.* **1967**, *89*, 1996.

(25) Schaver, C. K.; Anderson, O. P.; Eaton, S. S.; Eaton, G. R. *Inorg. Chem.* **1985**, *24*, 4082.

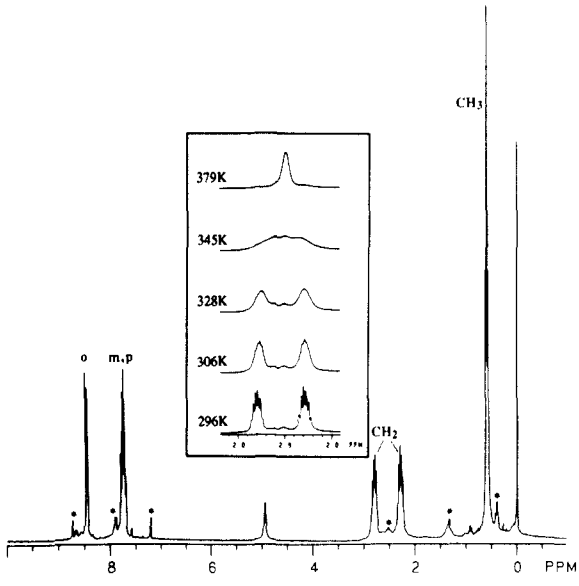

Figure 13. ^{1}H NMR spectrum of ZnOETPP in pyridine-d_5. Peak at 0 ppm is TMS. Peak at 5 ppm is water in the solvent. Starred peaks are trace impurities and the solvent. o, m, and p are the ortho, meta, and para phenyl protons, respectively. The inset illustrates the behavior of the methylene resonances as the temperature is raised.

crystallization at distances of 3.16 and 2.89 Å. Because the ZnOETPP molecules crystallize around a center of symmetry, OS1 and OS2 are further hydrogen-bonded to OS2 and OS1 of the inversion-related molecule, which is 2.96 Å away, to form an unusual six-membered oxygen ring (Figure 12). This arrangement can thus be described as successive hydrogen donation from each hydroxyl of the six-membered ring to its neighbor. The Zn atoms in the "dimers" are separated by 8.31 Å.

NMR Results

The obvious question arises whether the skeletal distortions observed in the crystals are retained in solution. The conformations of Zn and other OETPP complexes were therefore examined in solution by using high-field proton NMR spectroscopy. The ^{1}H NMR spectrum of ZnOETPP in pyridine-d_5 at room temperature consists of signals from the phenyl protons (H_{ortho} 8.44 ppm, $H_{meta/para}$ 7.74 ppm), and an ABX_3 pattern for the ethyl groups with the methyls at 0.59 ppm and two sets of methylenes at 2.83 and 2.24 ppm. The resonances are sharp, except for the methylene protons, which show some broadening at room temperature (Figure 13). Upon warming, the latter broaden further and coalesce at 345 K, meaning that they have become equivalent on the NMR time scale. Above the coalescence temperature, the methylene signal sharpens considerably but the boiling point of pyridine-d_5 prevents the observation of the expected well-resolved A_2X_3 pattern. The coalescence temperature, T_c, can be used to calculate the free energy of activation for the methylenes to become equivalent by using the standard equation,[26] $\Delta G^*/RT_c = 22.96 + \ln (T_c/\delta\nu)$, where $\delta\nu$ is the difference in the methylene resonances.

For a coalescence temperature of 345 K, this yields a value of $\Delta G^* = 16.2 \pm 0.2$ kcal mol^{-1}. Similar behaviors of the methylene groups are observed with several other OETPP derivatives with the following results: H_2OETPP, $\Delta G^*_{383} = 18.1 \pm 0.2$ kcal mol^{-1}; NiOETPP,[27] $\Delta G^*_{293} = 13.2 \pm 0.2$ kcal mol^{-1}; bispyridine Co^{III}·OETPP·OAc,[27] $\Delta G^*_{268} = 12.4 \pm 0.2$ kcal mol^{-1}.

The protonated dication, H_4OETPP^{2+}, shows no significant methylene broadening up to 407 K so that ΔG^* for this species must be greater than 20 kcal mol^{-1}. (Preliminary crystallographic results establish that H_4OETPP^{2+}·2OAc$^-$, H_2OETPP, and NiOETPP are also severely saddle-shaped.) In each of the above cases, the phenyl protons are unaffected by the dynamical processes at high temperatures. However, an additional process affects the spectrum of H_2OETPP, viz., N–H tautomerism which splits the methylene, methyl, ortho, and meta protons. These in turn coalesce at 293 K to yield $\Delta G^* = 13.7 \pm 0.2$ kcal mol^{-1}. For comparison, the barrier to N–H tautomerism in H_2TPP is reported[28] as 12.3 (^{13}C NMR) or 11.4 kcal mol^{-1} (^{1}H NMR). The phenyl protons of H_2TPP are unaffected, in contrast to the behavior observed for H_2OETPP, in which the ortho and meta protons split. If NH tautomerism is slow on the NMR time scale, the hydrogen atoms localize on trans pyrrole rings and the molecule retains 2-fold symmetry. If, in addition, the molecule is puckered, each face presents a different chemical environment and the ortho and meta protons become inequivalent, as observed. (The para protons lie in the plane of the porphyrin and are thus unaffected.)

The dynamic process observed for the methylene protons of all the OETPP complexes is particularly interesting, given the wide range of ΔG^* values. One possibility is that the ethyl groups are sterically crowded because of the adjacent phenyl rings so that rotation of the methylenes is hindered. However, this explanation does not account for the large differences in activation energy, given the similarities in X-ray structures. A more attractive alternative is a process whereby the porphyrin molecule inverts so that opposite pyrrole rings flip to the other side of the porphyrin plane and that the ethyl groups also flip to average the methylene groups. This mechanism is more consistent with the range of activation energies found as the occupancy of the porphyrin nitrogen pocket is changed. This effect would likely be most pronounced in the dication because of electrostatic and steric repulsions, as observed.

To confirm that porphyrin inversion and not ethyl rotation is indeed the process being observed, we synthesized a series of β-pyrrole-substituted tetraphenyl derivatives in which the β substituents are "tied back" to form cyclopentyl, cyclohexyl, and cycloheptyl rings.[27,29] In variable-temperature NMR experiments, the methylene protons of these complexes also coalesced, thereby providing further support for the idea that the porphyrin rings invert and that ethyl rotation is not the process being observed. This concept is not without precedent. Conformational inversion of a saddle-shaped Ni(II) octaethylpyrrocorphinate has been reported previously[30] as has the interconversion between "syn" and "anti" conformations of 5,15-dialkylporphyrins.[31] We conclude therefore that the macrocycle distortions observed crystallographically are retained in solution.

Discussion

Consequences and Implications of Puckering. The crystallographic results presented above illustrate some of the most severe distortions reported for porphyrins to date. Significant skeletal puckering has been observed in a variety of metalloporphyrins and in tetraaryl π cation radicals.[21] In Ni cases, macrocycle distortions are believed to result from the tendency to form short Ni–N bonds with a concomitant S_4 ruffling of the core.[5,21,30] In contrast to the ruffling induced by the small Ni ion, the large radius of Pb causes the metal to move significantly out of plane and the macrocycle assumes a "roof" shape.[32] For the tetraaryl π cation radicals, Scheidt and Lee[21] noted that all the saddle-shaped compounds reported are dimeric in the crystal and suggested that the skeletal distortions and rotations of the phenyl groups into the porphyrin plane serve to minimize steric repulsions and maximize porphyrin interactions. Clearly, in the present struc-

(26) Abraham, R. J.; Fisher, J.; Loftus, P. In *Introduction to NMR Spectroscopy*; Wiley and Sons: Chichester, England, 1988.
(27) For details of the syntheses, NMR, and optical spectra of these compounds, see: Medforth, C. J.; Berber, M. D.; Smith, K. M.; Shelnutt, J. A. *Tetrahedron Lett.* **1990**, *26*, 3719.
(28) Abraham, R. J.; Hawkes, G. E.; Smith, K. M. *Tetrahedron Lett.* **1974**, *16*, 1483.
(29) Preliminary X-ray results show Ni(II) tetracyclohexyltetraphenylporphyrin to be saddle-shaped.
(30) Waditschatka, R.; Kratky, C.; Jaun, B.; Heinzer, J.; Eschenmoser, A. *J. Chem. Soc., Chem. Commun.* **1985**, 1604.
(31) Maruyama, K.; Nagata, T.; Osuka, A. *J. Phys. Org. Chem.* **1988**, *1*, 63.
(32) Barkigia, K. M.; Fajer, J.; Adler, A. D.; Williams, G. J. B. *Inorg. Chem.* **1980**, *19*, 2057.

tures, the ruffling is not due to either the metal or dimerization and leads to the conclusion that the distortions help to minimize steric interactions between the meso- and β-carbon substituents. Preliminary crystallographic results for H_2OETPP, NiOETPP, and H_4OETPP·2OAc suggest the effect to be a general phenomenon for this type of porphyrin substitution. These conclusions are also consistent with CHARMM calculations[33] for the Zn complexes, which suggest that steric repulsions between the β and meso substituents account largely for the energy difference between planar and saddle-shaped porphyrins (~20 kcal mol^{-1} for ZnOETPP).

The consequences of the puckering on the properties of the nonplanar porphyrins are significant. We have previously noted that the absorption spectrum of ZnOETPP is red-shifted relative to either ZnTPP or ZnOEP. A similar effect is found for ZnOMTPP. INDO/s calculations[6] indicate that puckering destabilizes the π system of the macrocycle and principally raises the HOMO level with a smaller perturbation of the LUMO. The net result is a smaller energy gap between the HOMO and LUMO with a concomitant red shift of the first absorption band. In agreement with the calculations, ZnOETPP is easier to oxidize ($E_{1/2}$ = 0.47 V vs SCE in CH_2Cl_2) than either ZnTPP (0.75 V) or ZnOEP (0.63 V), whereas the reduction potentials in tetrahydrofuran are as follows: $E_{1/2}$ = −1.54, −1.35, and −1.63 V for ZnOETPP, ZnTPP, and ZnOEP, respectively.[6]

As is the case with *N*-alkylporphyrins,[34] the basicity of the puckered macrocycles also increases. The Zn complexes readily demetalate to the metal-free derivatives, and the latter form diacid compounds on addition of most protic solvents!

Equally interesting, besides the modulations of the optical and redox properties caused by the puckering, are the effects on the photophysics of the molecules. Melamed and Spiro[35] first called to our attention that H_2OETPP "did not fluoresce". In agreement with this observation, the fluorescence quantum yield of ZnOETPP is a factor of ~30 less than that of ZnTPP in benzene.[36,37]

As noted in the Introduction, an expanding body of structural information clearly demonstrates that porphinoid skeletons are flexible and that distortions of the macrocycles can be imposed by steric interactions in vitro and in vivo.[2-8,21] Some of the consequences of the porphyrin deformations on optical, redox, basicity, and excited-state properties have been noted here and had previously been invoked to explain magnetic interactions between paramagnetic metals and π cation radicals,[38] asymmetries in unpaired spin distributions in bacteriochlorophyll *b* cation radicals[11] and triplets,[12] distributions of states in bacterial reaction centers,[39] Fe d-orbital occupancies and CO binding in hemes,[40] and differences in binding of axial ligands and control of sites of reductions in Ni derivatives.[5,41] Clearly, conformational variations provide an attractive and simple mechanism for modulating a wide range of physical and chemical properties of porphyrin derivatives in vitro and in vivo. Such conformational effects can obviously be introduced by synthetic manipulations in vitro, and by a combination of axial ligation, hydrogen bonding, and nearby residues in vivo. Note also that if nearby residues of prosthetic groups help to define a structural scaffolding in vivo,[42] site-directed mutations may alter the protein pocket and indirectly affect the conformations and hence the properties of porphyrinic chromophores and prosthetic groups.

Acknowledgment. We thank J. S. Connolly, M. Gouterman, M. D. Newton, and T. G. Spiro for discussions and for communicating their results prior to publication. This work was supported by the Division of Chemical Sciences, U.S. Department of Energy, under Contract DE-AC02-76CH00016 at Brookhaven National Laboratory, and by National Science Foundation Grant CHE-86-19034 at the University of California, Davis. C.J.M. gratefully acknowledges a Fulbright Travel Scholarship.

Supplementary Material Available: For ZnOMTPP and ZnOETPP: Tables of final positional and anisotropic thermal parameters for the non-hydrogen atoms, final positional parameters for the hydrogen atoms, complete bond distances, bond angles, least-squares planes, torsion angles, and angles between rings, intramolecular contacts of phenyl groups, contact distances less than 4 Å, distances from the centers of the nitrogens, and contacts between ring centers (19 pages); observed and calculated structure factor amplitudes (35 pages). Ordering information is given on any current masthead page.

(33) Fajer, J.; Barkigia, K. M.; Zhong, E.; Gudowska-Nowak, E.; Newton, M. D. In *Structure and Function of Bacterial Reaction Centers*; Michel-Beyerle, M. E., Ed.; Springer-Verlag: Berlin, in press.

(34) Jackson, A. H. *Ann. N. Y. Acad. Sci.* **1973**, *206*, 151. Lavallee, D. K. The Chemistry and Biochemistry of N-Substituted Porphyrins; VCH: New York, 1987.

(35) Melamed, D.; Spiro, T. G., private communication.

(36) Fonda, H. N.; Connolly, J. S., private communication.

(37) The effects of peripheral substitutions and of the resulting conformational changes on excited states of porphyrins are under investigation. Possible explanations for these effects are changes in spin–orbit or vibronic coupling. The preliminary results raise a cautionary note about the use of fluorescence quenching as diagnostic of electron transfer in covalently linked porphyrin arrays.

(38) Erler, B. S.; Scholz, W. F.; Lee, Y.; Scheidt, W. R.; Reed, C. A. *J. Am. Chem. Soc.* **1987**, *109*, 2644.

(39) Kirmaier, C.; Holten, D. *Proc. Natl. Acad. Sci. U.S.A.* **1990**, *87*, 3552.

(40) Baltzer, L.; Landergren, M. *J. Am. Chem. Soc.* **1990**, *112*, 2804, and references therein.

(41) Alden, R. G.; Ondrias, M. R.; Shelnutt, J. A. *J. Am. Chem. Soc.* **1990**, *112*, 691. Furenlid, L. R.; Renner, M. W.; Smith, K. M.; Fajer, J. *J. Am. Chem. Soc.* **1990**, *112*, 1634, and references therein.

(42) Huber, R. *Eur. J. Biochem.* **1990**, *187*, 283.